


Circ_0000520 contributes to triple-negative breast cancer progression through mediating the miR-1296/ZFX axis

Yong Zhou | Guoxi Ma | Shijun Peng | Min Tuo | Yinmou Li | Xianxiong Qin | Qiang Yu | Sijie Kuang | Hong Cheng | Jing Li 

Department of Breast Surgery, The Central Hospital of Enshi Tujia and Miao Autonomous Prefecture, Enshi City, China

Correspondence

Jing Li, Department of Breast Surgery, The Central Hospital of Enshi Tujia and Miao Autonomous Prefecture, No.158 Wuyang Avenue, Enshi 445000, Hubei Province, China.
Email: ailxs841221@126.com

Abstract

Background: Triple-negative breast cancer (TNBC) is the most aggressive subtype of breast cancer with a high incidence of local recurrence and metastasis. Circular RNAs (circRNAs) are implicated in the pathomechanism of TNBC. Here, we investigated the function of circ_0000520 in TNBC and its associated mechanism.

Methods: Reverse transcription quantitative polymerase chain reaction (RT-qPCR) and Western blot assay were used to measure RNA and protein expression. Cell proliferation was analyzed by cell counting kit-8 (CCK8) assay, flow cytometry and colony formation assay. Cell apoptosis was assessed by flow cytometry. Cell migration ability was analyzed by transwell migration and wound healing assays. Transwell invasion assay was conducted to analyze the invasion ability. Dual-luciferase reporter assay, RNA immunoprecipitation (RIP) assay, and RNA-pulldown assay were performed to verify the interaction between microRNA-1296 (miR-1296) and circ_0000520 or zinc finger protein X-linked (ZFX). Xenograft mice model was established to analyze the role of circ_0000520 in xenograft tumor growth in vivo.

Results: Circ_0000520 expression was upregulated in TNBC tissues and cell lines. Circ_0000520 knockdown suppressed the proliferation, migration, and invasion whereas induced the apoptosis of TNBC cells. miR-1296 was verified as a target of circ_0000520, and circ_0000520 silencing-mediated suppressive effects on the malignant potential of TNBC cells were partly overturned by miR-1296 knockdown. miR-1296 interacted with the 3' untranslated region (3'UTR) of ZFX, and ZFX overexpression partly reversed miR-1296 overexpression-mediated effects in TNBC cells. Circ_0000520 absence reduced ZFX expression by upregulating miR-1296 in TNBC cells. Circ_0000520 silencing suppressed xenograft tumor growth in vivo.

Conclusions: Circ_0000520 contributed to TNBC development by binding to miR-1296 to induce ZFX expression.

KEYWORDS

circ_0000520, miR-1296, triple-negative breast cancer, ZFX

INTRODUCTION

Breast cancer is a common cancer among women, and is one of the leading causes of cancer-related death

globally.¹ Triple-negative breast cancer (TNBC) is featured by the absence of estrogen receptor (ER), human epidermal growth factor receptor 2 (HER2/neu), and progesterone receptor (PR).² The therapeutic methods for TNBC include surgery, chemotherapy, radiotherapy, and immunotherapy.³ Nevertheless, the prognosis of TNBC

Yong Zhou and Guoxi Ma contributed equally to this paper.

This is an open access article under the terms of the Creative Commons Attribution-NonCommercial-NoDerivs License, which permits use and distribution in any medium, provided the original work is properly cited, the use is non-commercial and no modifications or adaptations are made.

© 2021 The Authors. *Thoracic Cancer* published by China Lung Oncology Group and John Wiley & Sons Australia, Ltd.

patients at an advanced stage is still poor due to the high incidence of local recurrence and metastasis. Therefore, identifying novel targets is necessary for developing novel effective treatment strategies.

Circular RNAs (circRNAs) are featured by covalently linked terminals, high stability, abundant expression, and tissue-specific expression pattern, rendering them ideal biomarkers for the diagnosis, prognosis, and treatment of human diseases.^{4,5} CircRNAs have emerged as crucial regulators in many cancers.^{6,7} For instance, circ_001783 has been previously reported to be highly expressed in breast cancer tissues and cell lines, contributing to breast cancer development by serving as a molecular sponge for miR-200c-3p.⁸ A previous study reported that circ_0000520 level was decreased in gastric cancer, and circ_0000520 was found to be a potential biomarker for gastric cancer.⁹ Circ_0000520 expression was increased in TNBC tissues compared with nontumor tissues according to the dataset of GSE101124.¹⁰ However, the function of circ_0000520 in TNBC remains to be revealed.

CircRNAs play important regulatory roles in cancer initiation and progression through the networks of the competing endogenous RNAs (ceRNAs) to sponge target microRNAs (miRNAs) via base-pairing and modulate the downstream messenger RNAs (mRNAs) at the post-transcriptional level.^{11,12} The abnormal expression of miRNAs has been associated with the progression of many cancers.¹³ For example, miR-25-3p has been determined to facilitate the proliferation of TNBC cells through reducing BTG2 levels.¹⁴ Through bioinformatic prediction, miR-1296 has been found to be a potential target of circ_0000520. miR-1296 has been reported to suppress the proliferation of TNBC cells through targeting CCND1.¹⁵ Nevertheless, the working mechanism of miR-1296 in TNBC and its associated relationship with circ_0000520 are still largely unclear.

miRNAs can repress the translation or induce the degradation of target mRNAs through directly binding to them.¹⁶ Through bioinformatic analysis, it was found that the 3' untranslated region (3'UTR) of zinc finger protein X-linked (ZFX) possessed the complementary sites with miR-1296. ZFX has been determined to play an oncogenic role in pancreatic cancer,¹⁷ gastric cancer,¹⁸ renal carcinoma,¹⁹ and TNBC.²⁰ Han et al. demonstrated that CCAT1 contributed to the progression of TNBC through upregulating ZFX,²⁰ indicating the protumor role of ZFX in TNBC. Here, the signal regulatory network of ZFX in TNBC progression was investigated.

We first analyzed the expression pattern of circ_0000520 and found that circ_0000520 expression was markedly upregulated in TNBC tissues and cell lines. Loss-of-function experiments were conducted to analyze the biological function of circ_0000520 in TNBC cells. The working mechanism of circ_0000520 in TNBC progression was then explored through bioinformatic prediction and rescue experiments.

METHODS

Bioinformatic analysis

CircRNA expression profile in TNBC tissues ($n = 4$) and normal mammary gland tissue specimens ($n = 3$) was downloaded from the GSE101124 dataset. Circ_0000520/miRNAs interactions and miR-1296/mRNAs interactions were predicted by the Circinteractome database (<https://circinteractome.irp.nia.nih.gov/>) and StarBase database (<http://starbase.sysu.edu.cn>) on the basis of complementary sites.

Clinical samples

Fifty pairs of TNBC tissues and nontumor tissues from TNBC patients were collected in The Central Hospital of Enshi Tujia and Miao Autonomous Prefecture during surgical resection between February 2012 and July 2013. The protocol was authorized by the Ethics Committee of The Central Hospital of Enshi Tujia and Miao Autonomous Prefecture. Informed consent was provided by each participant before surgical resection. None of the patients had received chemotherapy or radiotherapy before surgery. These patients were followed for five years to generate a survival rate curve. The expression of circ_0000520, miR-1296 and ZFX was examined by reverse transcription quantitative polymerase chain reaction (RT-qPCR). The correlation between clinicopathological characteristics (from medical records) of TNBC patients and circ_0000520 expression level is shown in Table 1.

Hematoxylin–eosin (HE) staining

HE staining of TNBC tissue and adjacent normal tissue was performed according to the procedures of a previous study,²¹ and sections were visualized by a light microscopy with a magnification of 100 \times .

Cell lines

MCF-10A (human normal mammary cell line), MDA-MB-231 and BT549 were purchased from the Chinese Academy of Sciences Committee on Type Culture Collection Cell Bank (Shanghai, China). All cell lines were grown in Dulbecco's modified Eagle medium (DMEM, Gibco) added with 10% heat-inactivated fetal bovine serum (FBS, Gibco) and 1% penicillin–streptomycin (Gibco) in a humidified atmosphere with 5% CO₂ at 37°C.

Reverse transcription quantitative polymerase chain reaction (RT-qPCR)

Total RNA samples were extracted from tissues and cells with the TRIzol reagent (Invitrogen). Complementary DNA (cDNA)

TABLE 1 Correlation between clinicopathological characteristics of triple negative breast cancer (TNBC) patients and circ_0000520 expression level

Characteristics	circ_0000520		<i>p</i> -value
	High (<i>n</i> = 25)	Low (<i>n</i> = 25)	
Age (years)			
≥50	13	11	0.571
<50	12	14	
Menopause			
Yes	16	13	0.390
No	9	12	
TNM stage			
I + II	10	21	0.001*
III + IV	15	4	
Tumor size			
≤2.0 cm	10	18	0.023*
>2.0 cm	15	7	
Lymph node metastasis			
Positive	17	5	0.001*
Negative	8	20	

Note: TNM stage, tumor-node-metastasis stage; **p* < 0.05, statistically significant.

of circ_0000520 and ZFX was synthesized from 1 μg of RNA using the Bio-Rad iScript kit (Bio-Rad), and PCR was carried out with iQSYBR Green SuperMix (Bio-Rad) using cDNA as template DNA. Glyceraldehyde-3-phosphate dehydrogenase (GAPDH) was acted as the internal control for circ_0000520 or ZFX mRNA. To measure the abundance of miR-1296, cDNA was obtained using one step miRNA RT Kit (Haigene) followed by PCR reaction using TaqMan MicroRNA assay kit (Applied Biosystems). U6 served as the internal control for miR-1296. The relative levels of circ_0000520, miR-1296 and ZFX were analyzed using the $2^{-\Delta\Delta C_t}$ method. Primer sequences are listed in Table 2.

Cell transfection

Three small interfering RNAs targeting circ_0000520 (si-circ_0000520#1, si-circ_0000520#2 and si-circ_0000520#3), siRNA negative control (si-NC), short hairpin RNA against circ_0000520 (sh-circ_0000520) along with sh-NC were synthesized from Ribobio. miR-1296 mimic (miR-1296), miR-NC, miR-1296 inhibitor (anti-miR-1296) and anti-miR-NC were also obtained from Ribobio. pcDNA-ZFX and pcDNA were purchased from GenePharma. TNBC cells were transfected using Lipofectamine 3000 (Invitrogen), and the transfection efficiency was assessed via RT-qPCR.

Cell counting kit-8 (CCK8) assay

A total of 10 μl CCK8 reagent (Dojindo Molecular Technologies) was incubated with TNBC cells for 2 h at 0, 24, 48 or

72 h after transfection. The absorbance value at 450 nm wavelength was examined.

Flow cytometry

Flow cytometry was used for the detection of cell cycle progression and cell apoptosis.

TNBC cells were fixed in 70% cold ethanol solution overnight to analyze cell cycle progression. RNA content was removed using 10 μM RNase (Solarbio). DNA content was labeled by propidium iodide (PI; Solarbio) for 20 min. The percentages of TNBC cells in G0/G1, S or G2/M phase were analyzed by flow cytometer.

To analyze the apoptosis of TNBC cells, after transfection for 72 h, adherent TNBC cells along with nonadherent TNBC cells were harvested and resuspended using 400 μl binding buffer (BD Biosciences). Annexin V-fluorescein isothiocyanate (FITC; BD Biosciences) and PI (BD Biosciences) were simultaneously added into the reaction system to mark the phosphatidylserine and DNA content. The percentage of apoptotic TNBC cells (FITC⁺/PI^{+/-}) was analyzed by the flow cytometer.

Colony formation assay

Transfected TNBC cells were suspended in culture media at a low concentration, and cell suspension was added into 6-well plates at a density of 200 cells per well. These cells were routinely cultured for two weeks to form visible colonies. The colonies were fixed followed by staining using crystal violet (Sangon Biotech).

Transwell assays

The upper chambers (Costar) were coated (transwell invasion assay) or uncoated (transwell migration assay) with Matrigel (Sigma). A total of 100 μl cell suspension (serum-free medium) was added into the coated or uncoated upper chambers, and 600 μl culture medium plus 10% FBS (chemotactic factor) were added to the lower chambers. After 24-h incubation, TNBC cells which remained on the upper surface of the membrane were removed, and the invaded or migrated TNBC cells were fixed and counted. Magnification time: 100 × .

Wound healing assay

Transfected TNBC cells continued to be cultured until the confluence reached about 90%. A wound was generated using a 200 μl pipette tip to scratch the cell monolayer. Cell debris was removed through washing three times with phosphate buffered saline (PBS). Cells were cultured for 24 h, and the scratch images were obtained with an inverted microscope (40×, Olympus).

TABLE 2 Primers in RT-qPCR assay

Gene	Species	Direction	Sequence (5'-3')
circ_0000520	Human	Forward	GGGAAGGTCTGAGACTAGGG
		Reverse	GGACATGGGAGTGGAGTGAC
miR-1296	Human	Forward	TTGTTAGGGCCCTGGCTC
		Reverse	CAGTGCAGGGTCCGAGGTAT
ZFX	Human	Forward	GGCAGTCCACAGCAAGAAC
		Reverse	TTGGTATCCGAGAAAG TCAGAAG
GAPDH	Human	Forward	TATGATGACATCAAGAA GGTGGT
		Reverse	TGTAGCCAAATTCGTTGTCATAC
U6	Human	Forward	GCTTCGGCAGCACATA TACTAAAAT
		Reverse	CGCTTCACGAATTTG CGTGTCAT

Dual-luciferase reporter assay

Dual-luciferase reporter assay was performed to verify the interaction between miR-1296 and circ_0000520 or ZFX in TNBC cells.

The fragment of circ_0000520 or ZFX 3'UTR harboring the wild-type binding sites with miR-1296 was amplified and cloned to pmiRGLO vector (Promega), termed as circ_0000520-WT or ZFX 3'UTR-WT. The partial sequence of circ_0000520 or ZFX 3' untranslated region (3'UTR) containing the mutant type binding sites with miR-1296 was also cloned to pmiRGLO vector (Promega) to obtain circ_0000520-MUT or ZFX 3'UTR-MUT. The luciferase plasmids (50 ng) were transfected into TNBC cells with miR-NC or miR-1296 (20 nM) for 24 h. Luciferase activities (Firefly and Renilla) in different groups were detected with dual-luciferase reporter assay system (Promega).

RNA immunoprecipitation (RIP) assay

Magnetic beads were incubated with Argonaute-2 (Ago2) antibody (Anti-Ago2; Abcam) or immunoglobulin G (IgG) antibody (Anti-IgG; Abcam). After disrupting with RIP lysis buffer (Millipore) plus RNase inhibitor (Millipore), cell lysates were divided into two equal parts and incubated with the precoated magnetic beads. RT-qPCR was implemented to detect the expression of circ_0000520, miR-1296 and ZFX mRNA.

RNA-pulldown assay

miR-1296 was biotinylated to generate Bio-miR-1296. Bio-NC was used as the control. Cell lysate was incubated with

Bio-NC or Bio-miR-1296. The expression of circ_0000520 was detected by RT-qPCR.

Western blot assay

TNBC cells were disrupted in radioimmunoprecipitation assay (RIPA) buffer (Beyotime). A total of 25 µg of protein samples were loaded onto sodium dodecyl sulfate polyacrylamide gel electrophoresis (SDS-PAGE) gel at 100 V for 120 min followed by electrotransfer onto polyvinylidene fluoride (PVDF) membrane (Millipore). The membrane was blocked using 5% skimmed milk for 1 h prior to incubation with primary antibodies at 4°C overnight. The primary antibodies included anti-ZFX (ab246858; Abcam) and anti-GAPDH (ab8245; Abcam). The membrane was then probed with horseradish peroxidase (HRP)-conjugated secondary antibody (Abcam). The protein bands were measured with the an enhanced chemiluminescence kit (GE Healthcare).

Xenograft tumor assay

Animal experiments were performed with the authorization of the Animal Research Committee of The Central Hospital of Enshi Tujia and Miao Autonomous Prefecture. BALB/c nude mice (Orient Bio Inc) were arbitrarily divided into two groups ($n = 7$). The stable circ_0000520 silencing MDA-MB-231 cell line was built using sh-circ_0000520. An MDA-MB-231 cell line stably transfected with sh-NC was used as the control. MDA-MB-231 cells suspended in 200 µl PBS were subcutaneously inoculated into the back of mice. After inoculation for seven days, the tumor length and width were detected weekly, and the tumor volume was calculated by the formula of $\text{length} \times \text{width}^2 \times \pi/6$. Tumors were excised and weighed at 35 days after inoculation. RT-qPCR was implemented to detect the expression of circ_0000520, miR-1296 and ZFX mRNA, while the protein expression of ZFX was examined by Western blot assay.

Statistical analysis

The results are displayed as mean \pm standard deviation (SD). Data were analyzed for the normality using the D'Agostino-Pearson omnibus normality test and homogeneity of variances using the Levene test. For normally distributed data with equal variance, the comparison in two groups or multiple groups was assessed using Student's *t*-test or one-way analysis of variance (ANOVA) followed by Tukey's test. Linear correlation relationship was analyzed using Spearman's correlation coefficient. Kaplan-Meier plot survival curve was analyzed using log-rank test. The correlation between clinicopathological characteristics of TNBC patients and circ_0000520 expression level was analyzed by χ^2 test. Statistical analysis was conducted using the Prism 7.0

(GraphPad Software). $p < 0.05$ was identified to be statistically significant.

RESULTS

Circ_0000520 absence suppresses the proliferation, migration, and invasion and induces the apoptosis of TNBC cells

The top 10 most up- and downregulated circRNAs in TNBC tissue specimens ($n = 4$) compared with normal mammary gland tissue specimens ($n = 3$) according to GSE101124 dataset were shown in Figure 1(a). It was found that circ_0000520 was significantly upregulated in TNBC tissues compared with normal tissues (Figure 1(b)). Circ_0000520 is a short circRNA with 123 bp that generated from the exon1 of *RPPH1* gene (Figure 1(c)). The back-splicing sites (AG-GG) and mature sequence of circ_0000520 are also shown in Figure 1(c). We collected 50 TNBC tissue samples and corresponding adjacent normal tissues for pathological diagnosis and RT-qPCR analysis. As shown in Figure 1(d), representative images of HE staining are displayed. Circ_0000520 expression was significantly upregulated in TNBC tissues compared with adjacent normal tissues (Figure 1(e)). TNBC patients were divided into high and low expression groups with a median value of circ_0000520 expression as the cutoff. The Kaplan–Meier survival curve revealed that TNBC patients with high expression of circ_0000520 were associated with shorter survival time (Figure 1(f)). These results demonstrated that high expression circ_0000520 might be an unfavorable indicator for TNBC patients.

We measured the expression of circ_0000520 in human normal mammary epithelial cell line MCF-10A and two TNBC cell lines (MDA-MB-231 and BT549) via RT-qPCR. As shown in Figure 1(g), Circ_0000520 was upregulated in TNBC cell lines compared with MCF-10A cell lines. Three small interfering RNAs targeting the back-splicing sites of circ_0000520 were designed to specifically silence circ_0000520 in TNBC cells. Prior to functional experiments, we assessed the knockdown efficiencies of three siRNAs in TNBC cells. Circ_0000520 expression was significantly reduced in all three groups, especially in the si-circ_0000520#2 group (Figure 1(h)). Therefore, si-circ_0000520#2 was chosen for functional experiments. We analyzed the proliferation of TNBC cells by CCK8 assay, flow cytometry, and colony formation assay. The proliferation of TNBC cells was suppressed by the silence of circ_0000520 (Figure 1(i) and (j)). Flow cytometry showed that circ_0000520 knockdown arrested cell cycle progression at G1/S transition (Figure 1(k) and (l)). The number of colonies was reduced in the si-circ_0000520#2 group (Figure 1(m)), demonstrating that circ_0000520 silencing suppressed the proliferation of TNBC cells. Furthermore, circ_0000520 silencing induced the apoptosis of TNBC cells (Figure 1(n)). We also analyzed the influences of circ_0000520 interference on the migration and invasion of TNBC cells via

transwell and wound healing assays. Transwell assays revealed that the numbers of migrated and invaded TNBC cells were both reduced in circ_0000520-silenced group compared with the si-NC group (Figure 1(o) and (p)). Wound healing assay revealed that circ_0000520 absence markedly reduced the rate of wound closure (Figure 1(q)), suggesting that circ_0000520 knockdown restrained the migration ability of TNBC cells. Overall, circ_0000520 knockdown suppressed the proliferation, migration, and invasion and induced the apoptosis of TNBC cells.

miR-1296 is a target of circ_0000520 in TNBC cells

CircRNAs can regulate cell biological behaviors by acting as miRNA sponges.¹¹ To further explore the working mechanism of circ_0000520, we conducted bioinformatic analysis using the Circinteractome database to seek the interacted miRNAs of circ_0000520. The putative binding sites between miR-1296 and circ_0000520 were shown in Figure 2(a). High overexpression efficiency of miR-1296 mimic was confirmed by RT-qPCR (Figure 2(b)). Subsequently, we performed dual-luciferase reporter, RIP and RNA-pulldown assays to verify the target relationship between miR-1296 and circ_0000520. miR-1296 overexpression markedly reduced the luciferase activity of wild-type luciferase plasmid (circ_0000520-WT) rather than mutant plasmid (circ_0000520-MUT) (Figure 2(c) and (d)), suggesting that circ_0000520 interacted with miR-1296 via the putative sequence. As shown in Figure 2(e) and (f), circ_0000520 and miR-1296 were both enriched in Anti-Ago2 group compared with the Anti-IgG group, suggesting a spatial interaction between circ_0000520 and miR-1296 in RNA-induced silencing complex (RISC). Circ_0000520 was pulled down when using Bio-miR-1296 rather than Bio-NC (Figure 2(g)), suggesting that miR-1296 bound to circ_0000520 in TNBC cells. Circ_0000520 knockdown significantly upregulated miR-1296 expression in TNBC cells (Figure 2(h)). As shown in Figures 2(i) and (j), miR-1296 expression was notably reduced in TNBC tissues and cell lines compared with normal tissues and MCF-10A cell line. Overall, these results indicated that circ_0000520 negatively regulated miR-1296 level by directly binding to it in TNBC cells.

To investigate whether circ_0000520 regulated the biological behaviors of TNBC cells by sponging miR-1296, we cotransfected TNBC cells with si-NC, si-circ_0000520#2, si-circ_0000520#2 + anti-miR-NC, or si-circ_0000520#2 + anti-miR-1296 to conduct rescue experiments. The silencing efficiency of anti-miR-1296 was analyzed via RT-qPCR. The transfection of anti-miR-1296 notably decreased the expression of miR-1296 (Figure 2(k)), suggesting that anti-miR-1296 was effective in silencing miR-1296 in TNBC cells. miR-1296 interference largely overturned si-circ_0000520-mediated suppressive effect on the proliferation of TNBC cells (Figure 2(l) and (m)). Circ_0000520 knockdown-induced cell cycle arrest in TNBC cells was partly alleviated by anti-miR-1296

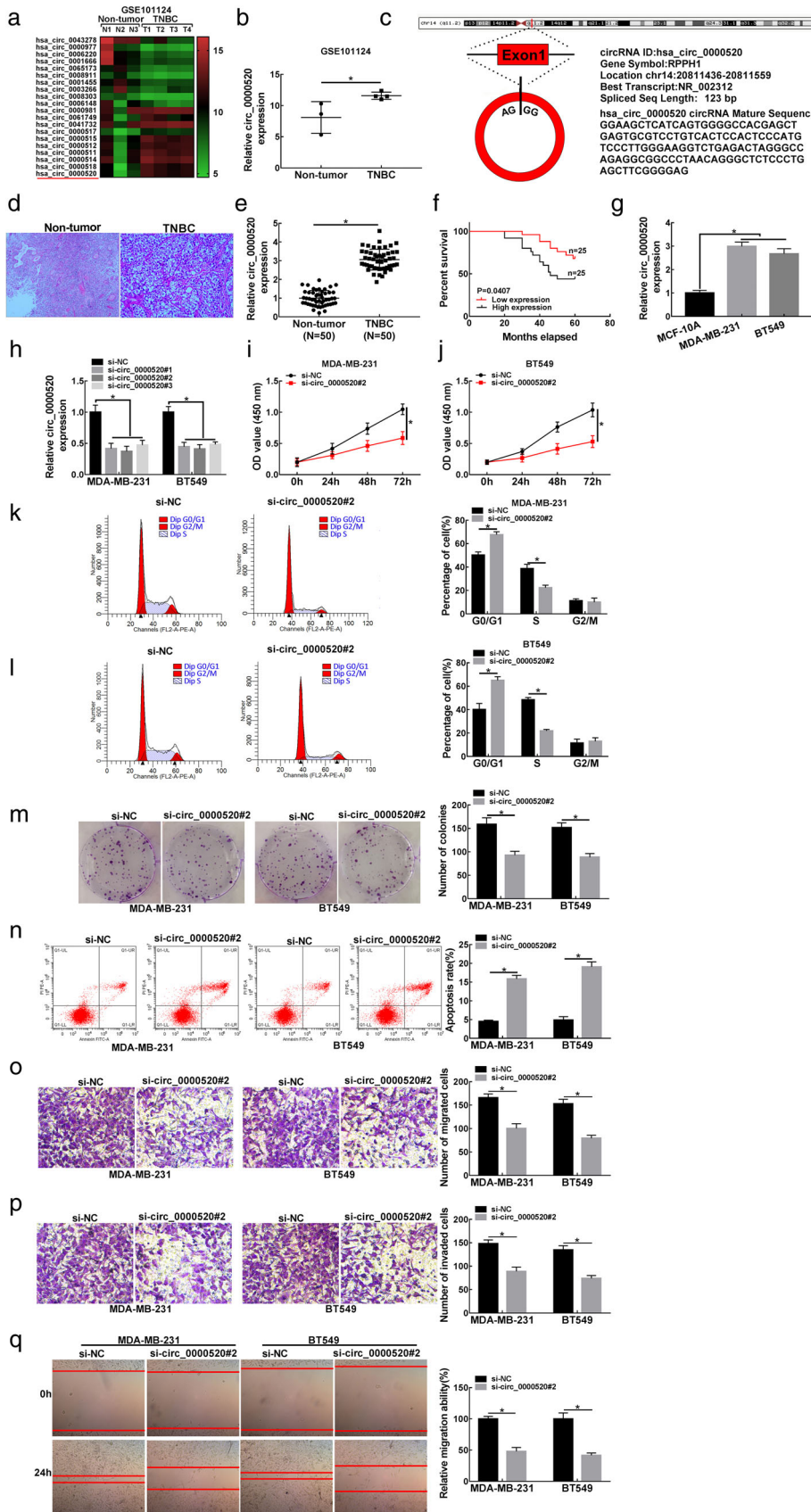


FIGURE 1 Circ_0000520 absence suppresses the proliferation, migration, and invasion and induces the apoptosis of TNBC cells. (a) The top 10 most upregulated and downregulated circRNAs in TNBC tissue specimens ($n = 4$) compared with normal mammary gland tissue specimens ($n = 3$) were displayed in the heatmap. (b) The expression of circ_0000520 in TNBC tissues ($n = 4$) and normal tissues ($n = 3$) according to the data of GSE101124 was shown. (c) Circ_0000520 was generated from the back-splicing of exon1 in *RPPH1* gene, and its mature sequence was shown. (d) The representative images of HE staining in adjacent normal tissue and TNBC tissue were shown. (e) RT-qPCR was implemented to measure the expression of circ_0000520 in TNBC tissue samples ($n = 50$) and adjacent normal tissue samples ($n = 50$). (f) The 5-year survival rate of TNBC patients with high expression or low expression of circ_0000520 was analyzed by log-rank test. (g) Circ_0000520 level in MCF-10A and two TNBC cell lines (MDA-MB-231 and BT549) was examined by RT-qPCR. (h) Circ_0000520 expression in MDA-MB-231 or BT549 cells transfected with si-circ_0000520#1, si-circ_0000520#2, si-circ_0000520#3 or si-NC was analyzed by RT-qPCR. (i-n) MDA-MB-231 or BT549 cells were transfected with si-circ_0000520#2 or si-NC. (i and j) Cell proliferation was assessed by CCK8 assay. (k and l) TNBC cells in different phases of cell cycle (G0/G1, S and G2/M) were identified using flow cytometry. (m) The number of visible colonies of TNBC cells with circ_0000520 silencing or not was analyzed by colony formation assay. (n) Flow cytometry was used to assess the apoptosis rate in si-circ_0000520#2 transfected group or si-NC group. (o-q) MDA-MB-231 and BT549 cells were transfected with si-NC or si-circ_0000520#2. (o and p) The migration ability and invasion capacity in TNBC cells were evaluated using transwell assays. (q) Cell migration ability was assessed by wound healing assay. * $p < 0.05$

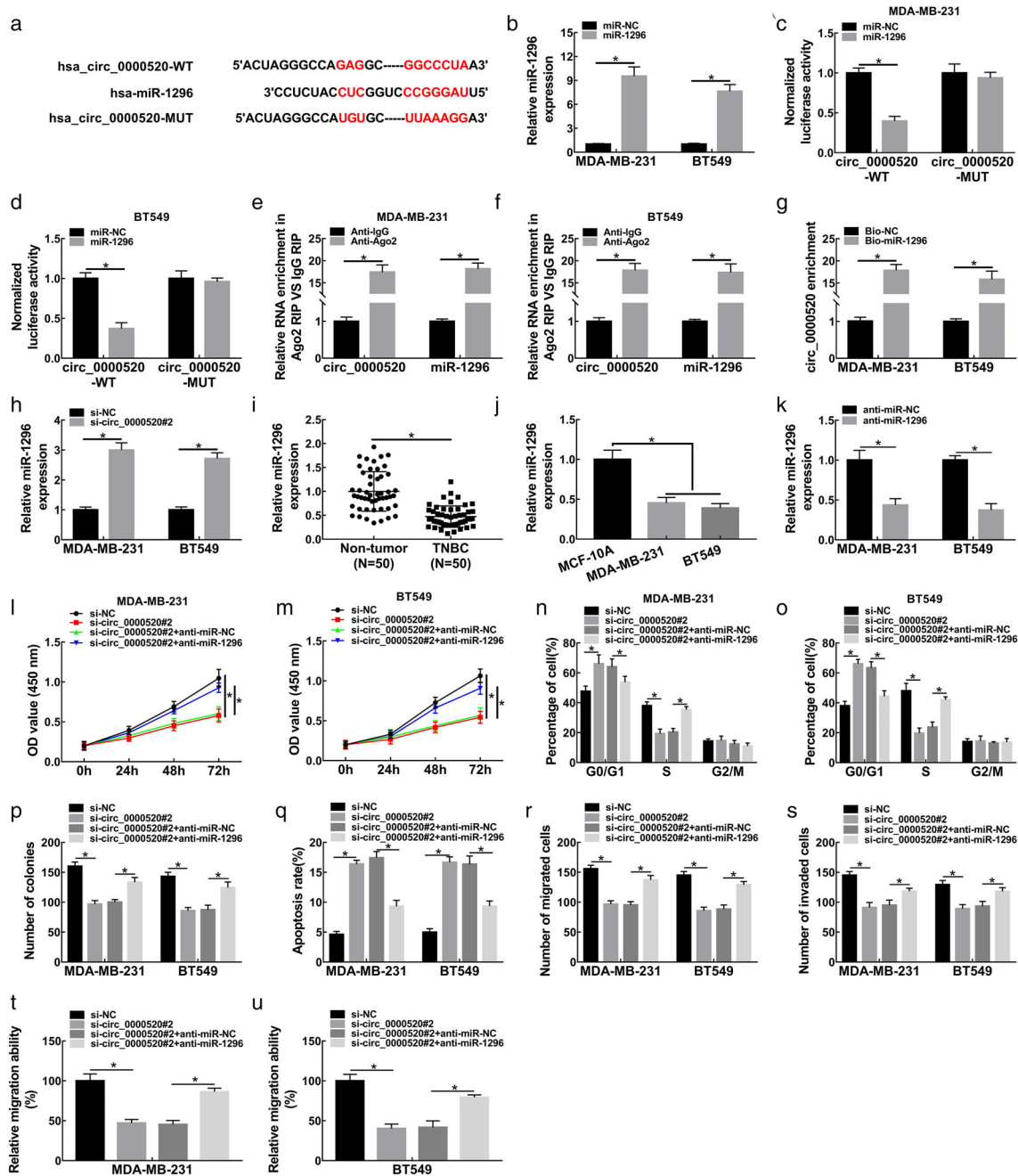


FIGURE 2 miR-1296 is a target of circ_0000520 in TNBC cells. (a) Circ_0000520-miRNAs interactions were explored using Circinteractome bioinformatics online database. miR-1296 was predicted as a candidate molecular target of circ_0000520, and the putative binding sites between miR-1296 and circ_0000520 were shown. (b) miR-1296 expression in TNBC cells transfected with miR-NC or miR-1296 was detected by RT-qPCR. (c and d) Dual-luciferase reporter assay was conducted to test the target interaction between miR-1296 and circ_0000520 in TNBC cells. Luciferase activity was examined in TNBC cells co-transfected with miR-NC or miR-1296 and circ_0000520-WT or circ_0000520-MUT. (e and f) RIP assay was utilized to evaluate the binding relationship between miR-1296 and circ_0000520 in TNBC cells. (g) RNA-pulldown assay was performed to test if miR-1296 bound to circ_0000520 in TNBC cells. (h) The regulatory relationship between miR-1296 and circ_0000520 was analyzed by RT-qPCR. (i) miR-1296 expression in TNBC tissues ($n = 50$) and adjacent normal tissues was analyzed using RT-qPCR. (j) miR-1296 abundance was measured in MCF-10A, MDA-MB-231 and BT549 cells by RT-qPCR. (k) The transfection efficiency of anti-miR-1296 was evaluated by RT-qPCR. (l–u) MDA-MB-231 and BT549 cells were transfected with the following four groups: Si-NC, si-circ_0000520#2, si-circ_0000520#2 + anti-miR-NC or si-circ_0000520#2 + anti-miR-1296. (l and m) CCK8 assay was carried out to analyze the proliferation capacity of TNBC cells. (n and o) The percentage of TNBC cells in G0/G1, S or G2/M phase was analyzed by flow cytometry. (p) Colony formation assay was conducted to measure the colony formation ability of TNBC cells. (q) Apoptotic TNBC cells in early stage and late stage were distinguished from normal or necrotic TNBC cells by flow cytometry, and the apoptosis rate was counted. (r and s) The migration and invasion capacities were measured by transwell assays. (t and u) Wound healing assay was carried out to analyze the migration ability of TNBC cells. * $p < 0.05$

(Figure 2(n) and (o)). The colony formation ability was partly recovered in si-circ_0000520#2 and anti-miR-1296 co-transfected group (Figure 2(p)). miR-1296 knockdown attenuated circ_0000520 absence-induced apoptosis in TNBC cells (Figure 2(q)). Circ_0000520 silencing-induced suppressive effects on the migration and invasion of TNBC cells were partly counteracted by anti-miR-1296 (Figure 2(r) and (s)). Wound healing assay showed that anti-miR-1296 partly regained the migration ability in circ_0000520-silenced TNBC cells (Figure 2(t) and (u)). These findings demonstrated that circ_0000520 silencing suppressed the malignant behaviors of TNBC cells partly by upregulating miR-1296.

miR-1296 binds to the 3'UTR of ZFX mRNA in TNBC cells

miRNAs can suppress the translation or induce the degradation of target mRNAs by binding to their 3'UTR.¹⁶ ZFX was predicted as a possible target of miR-1296 via StarBase

database (Figure 3(a)). Luciferase activity was markedly reduced in ZFX 3'UTR-WT group when cotransfected with miR-1296 rather than miR-NC, and the transfection of miR-NC or miR-1296 had no significant influence in the luciferase activity of ZFX 3'UTR-MUT group (Figure 3(b) and (c)), suggesting that miR-1296 interacted with ZFX 3'UTR via the putative binding sites. RIP assay showed that ZFX bound to miR-1296 in RISC (Figure 3(d) and (e)). The results of dual-luciferase reporter assay and RIP assay together demonstrated that ZFX was a target of miR-1296 in TNBC cells. We overexpressed or silenced miR-1296 with miR-1296 mimic or anti-miR-1296 to test the regulatory relationship between miR-1296 and ZFX in TNBC cells. As shown in Figure 3(f) and (g), miR-1296 overexpression significantly reduced ZFX mRNA and protein expression, whereas miR-1296 silencing markedly upregulated ZFX mRNA and protein levels in TNBC cells. ZFX mRNA and protein expression was notably upregulated in TNBC tissues compared with adjacent non-tumor tissues (Figure 3(h) and (i)). ZFX mRNA and protein levels were also elevated in MDA-MB-231 and BT549

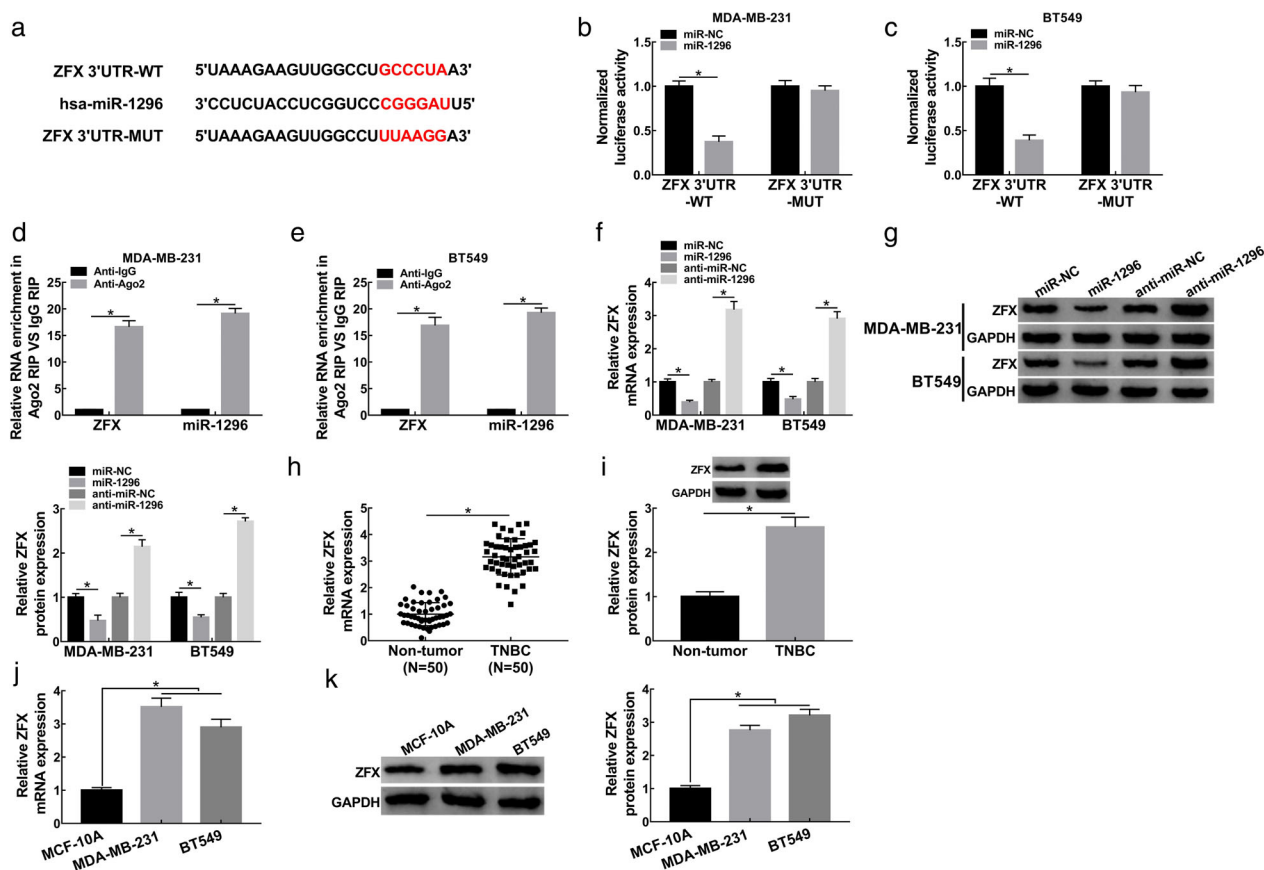


FIGURE 3 miR-1296 binds to the 3'UTR of ZFX mRNA in TNBC cells. (a) StarBase bioinformatics online database was used to predict miR-1296-mRNA interactions. The putative target sites between ZFX and miR-1296 were listed, and the mutant binding sites with miR-1296 in ZFX were also listed. (b and c) Dual-luciferase reporter assay was implemented to explore if the 3'UTR of ZFX interacted with miR-1296 via its "GCCCUA" sequence. (d and e) RIP assay was conducted to test the interaction between miR-1296 and ZFX mRNA in TNBC cells. (f and g) The mRNA and protein expression of ZFX in TNBC cells transfected with miR-NC, miR-1296, anti-miR-NC or anti-miR-1296 was examined by RT-qPCR and Western blot assay. (h and i) The mRNA and protein abundance of ZFX in TNBC tissues and normal tissues was measured by RT-qPCR and Western blot assay. (j and k) RT-qPCR and Western blot assay were conducted to analyze the mRNA and protein expression of ZFX in TNBC cell lines and MCF-10A cell line. * $p < 0.05$

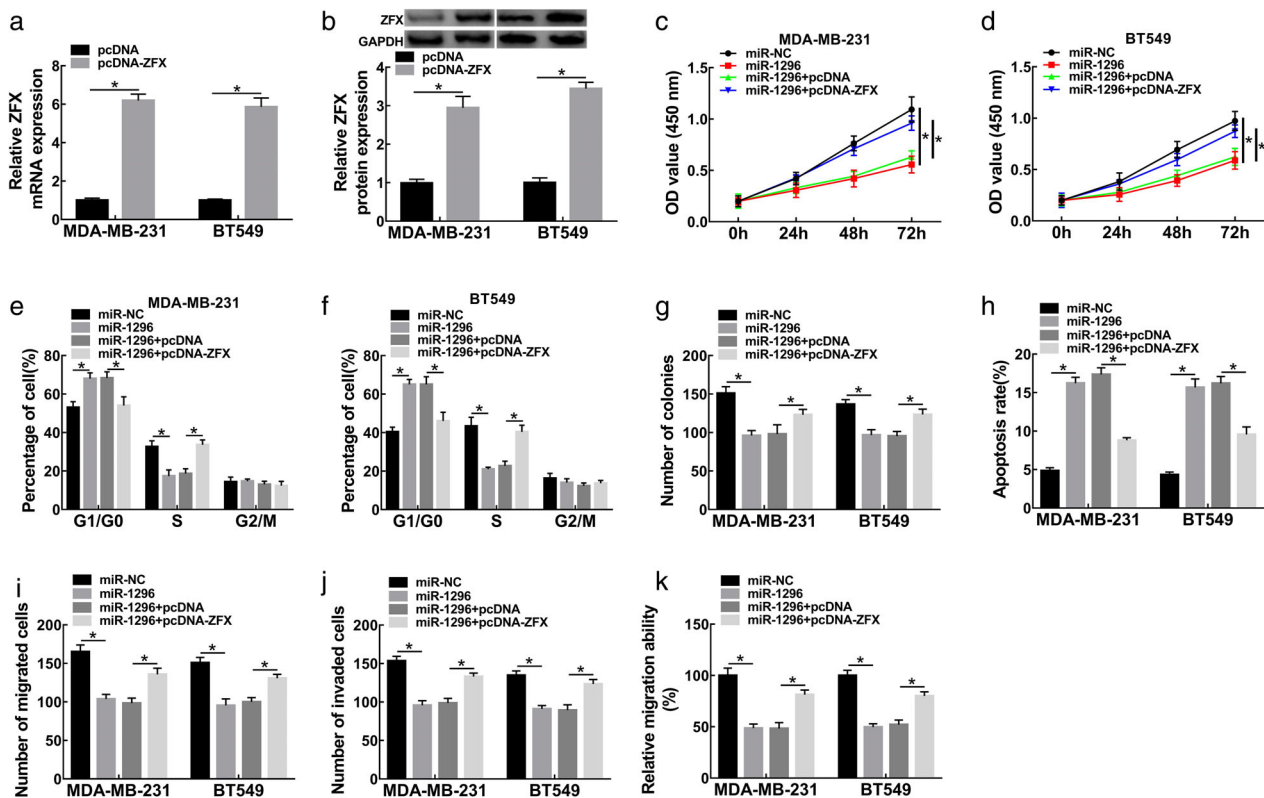


FIGURE 4 miR-1296 overexpression suppresses the malignant potential of TNBC cells partly by downregulating ZFX level. (a and b) The mRNA and protein expression of ZFX in TNBC cells transfected with pcDNA or pcDNA-ZFX was measured by RT-qPCR and Western blot assay. (c–k) TNBC cells were transfected with miR-NC, miR-1296, miR-1296 + pcDNA or miR-1296 + pcDNA-ZFX. (c and d) CCK8 assay was utilized to assess the proliferation ability in four groups. (e and f) Cell cycle progression was evaluated by flow cytometry. (g) Colony formation ability was evaluated by colony formation assay. (h) The apoptosis rate in four groups was analyzed by flow cytometry. (i and j) Transwell assays were performed to analyze the migration and invasion abilities of TNBC cells. (k) The migration ability of TNBC cells was analyzed by wound healing assay. * $p < 0.05$

cell lines compared with MCF-10A cell line (Figure 3 (j) and (k)). Taken together, ZFX was a molecular target of miR-1296, and ZFX was negatively regulated by miR-1296 in TNBC cells.

miR-1296 overexpression suppresses the malignant potential of TNBC cells partly by downregulating ZFX level

The transfection efficiency of pcDNA-ZFX was high, evidenced by the increased mRNA and protein levels of ZFX in TNBC cells transfected with pcDNA-ZFX (Figure 4(a) and (b)). In order to explore whether miR-1296 functioned by targeting ZFX, we performed rescue experiments through transfecting miR-1296 alone or together with pcDNA-ZFX into TNBC cells. miR-1296 overexpression suppressed the proliferation, migration, and invasion and promoted apoptosis of TNBC cells (Figure 4(c)–(k)), which further confirmed that miR-1296 acted as a tumor suppressor in TNBC. The addition of pcDNA-ZFX largely recovered the proliferation ability of TNBC cells (Figure 4(c)–(g)). miR-1296 overexpression-induced apoptosis was largely attenuated in miR-1296

and pcDNA-ZFX cotransfected group (Figure 4(h)). According to the transwell assay results, miR-1296-mediated suppressive effects on the migration and invasion of TNBC cells were both attenuated by the addition of pcDNA-ZFX (Figure 4(i) and (j)). Wound healing assay verified that ZFX overexpression partly restored the migration ability in miR-1296-overexpressed TNBC cells (Figure 4(k)). These results demonstrated that miR-1296 suppressed the progression of TNBC partly through downregulating ZFX in vitro.

ZFX regulated by circ_0000520/miR-1296 axis in TNBC cells

MDA-MB-231 and BT549 cells were transfected with si-NC, si-circ_0000520#2, si-circ_0000520#2 + anti-miR-NC, or si-circ_0000520#2 + anti-miR-1296. The mRNA and protein expression of ZFX was examined via RT-qPCR and Western blot assay. Circ_0000520 interference notably decreased ZFX mRNA and protein expression, and the addition of anti-miR-1296 partly regained the mRNA and protein levels of ZFX in TNBC cells (Figure 5(a) and (b)). Spearman's correlation coefficient was used to analyze the linear relationship among circ_0000520, miR-1296, and ZFX in TNBC

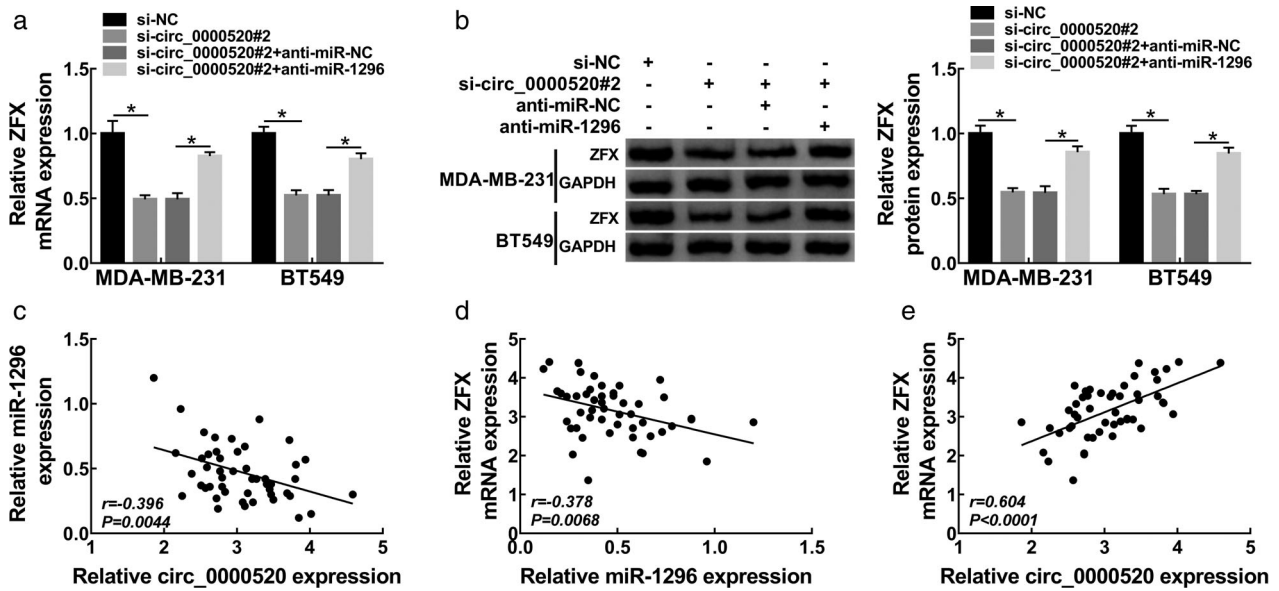


FIGURE 5 ZFX is regulated by circ_0000520/miR-1296 axis in TNBC cells. (a and b) TNBC cells were transfected with si-NC, si-circ_0000520#2, si-circ_0000520#2 + anti-miR-NC or si-circ_0000520#2 + anti-miR-1296. The mRNA and protein abundance of ZFX in TNBC cells was analyzed using RT-qPCR and Western blot assay. (c–e) The linear relationship among circ_0000520, miR-1296 and ZFX was analyzed by Spearman's correlation coefficient. * $p < 0.05$

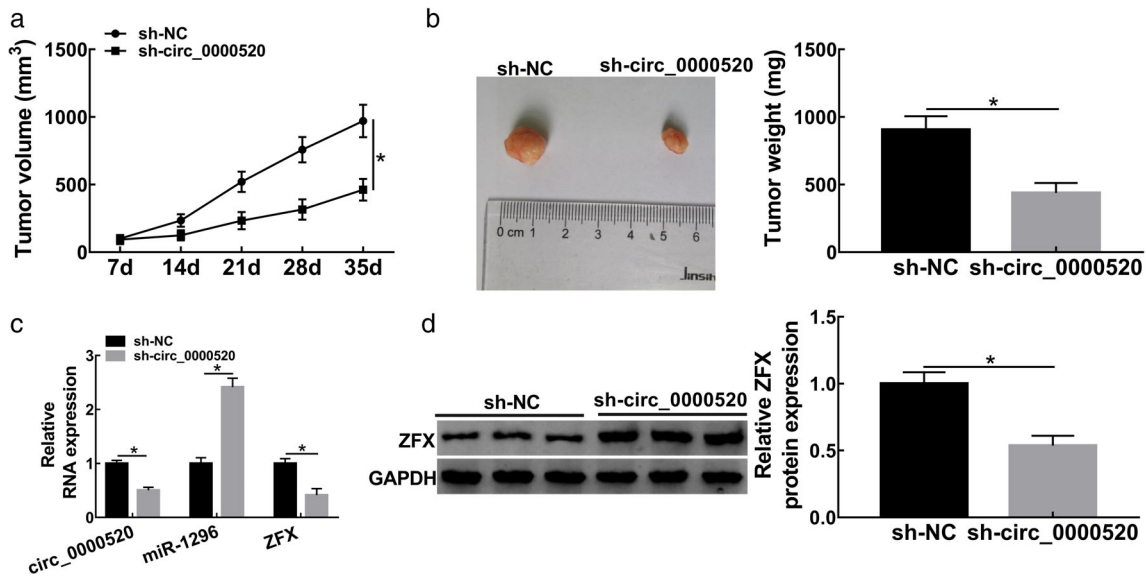


FIGURE 6 Circ_0000520 knockdown suppresses xenograft tumor growth in vivo. (a) The length and width of tumors in sh-NC group and sh-circ_0000520 group were measured every week, and tumor volume was calculated by length \times width² \times $\pi/6$. (b) Tumors were resected after 35 day inoculation, and tumor weight in two groups was measured. (c and d) RT-qPCR and Western blot assay were performed to detect the expression of circ_0000520, miR-1296 and ZFX mRNA and protein in tumor tissues. * $p < 0.05$

cells. miR-1296 expression was negatively correlated with the expression of circ_0000520 or ZFX mRNA (Figure 5 (c) and (d)), whereas there was a positive linear correlation between the expression of circ_0000520 and ZFX (Figure 5(e)). Accordingly, we concluded that circ_0000520 sponged miR-1296 to enhance ZFX expression in TNBC cells.

Circ_0000520 knockdown suppresses xenograft tumor growth in vivo

Given the results that circ_0000520 promoted the malignant behaviors of TNBC cells in vitro, we then explored the role of circ_0000520 on the growth of xenograft tumors in vivo. MDA-MB-231 cell line stably transfected with sh-NC or sh-

circ_0000520 was established to conduct xenograft tumor assay. Circ_0000520 silencing notably suppressed tumor growth (Figure 6(a) and (b)). The expression of circ_0000520 and ZFX mRNA and protein was reduced in tumor tissues in sh-circ_0000520 group compared with sh-NC group (Figure 6 (c) and (d)). In addition, miR-1296 expression was up-regulated in tumor tissues in sh-circ_0000520 group compared with sh-NC group (Figure 6(c)). Taken together, circ_0000520 absence inhibited xenograft tumor growth in vivo.

DISCUSSION

Accumulating evidence pointed out that circRNAs were widely dysregulated in human cancers.^{6,22,23} Due to the stable circular structure, circRNAs are ideal biomarkers for human cancers.^{23,24} Nevertheless, little is known about the roles and functions of circRNAs in TNBC. Circ-ITCH was downregulated in TNBC, and circ-ITCH restrained the proliferation and motility of TNBC cells by sponging miR-214 and miR-17.²⁵ Circ-UBAP2 was upregulated in TNBC, and circ-UBAP2 contributed to TNBC progression through regulating miR-661/MTA1 signaling.²⁶ On the basis of the data of GSE101124, circ_0000520 was upregulated in TNBC. Consistent with the above results, we found that circ_0000520 level was elevated in TNBC tissues compared with adjacent nontumor tissues. Loss of function experiments revealed that circ_0000520 silencing suppressed the proliferation and motility and induced the apoptosis of TNBC cells.

CircRNAs regulate the expression of downstream mRNAs through sponging miRNAs, which is also known as competing endogenous RNA (ceRNA) mechanism.^{27,28} For instance, circ-BPTF facilitated the development and recurrence of bladder cancer through upregulating RAB27A via sponging miR-31-5p.²⁹ To gain a better understanding of the working mechanism of circ_0000520 in TNBC, the Circinteractome bioinformatics database was used to seek the candidate miRNA targets of circ_0000520. Among the candidate miRNA targets of circ_0000520, miR-1296 was chosen for further analysis due to its tumor suppressor role in many malignancies.^{15,30–32} For example, miR-1296 suppressed the motility and epithelial-mesenchymal transition of hepatocellular carcinoma cells.³² Phan et al. found that miR-1296 hampered the proliferation of TNBC cells by downregulating CCND1.¹⁵ The target interaction between circ_0000520 and miR-1296 in TNBC cells was subsequently confirmed. miR-1296 was negatively regulated by circ_0000520 in TNBC cells, and miR-1296 expression was notably reduced in TNBC tissues and cell lines. Circ_0000520 absence-induced influences are largely overturned by the addition of anti-miR-1296 in TNBC cells, suggesting that circ_0000520 promoted the malignant behaviors of TNBC cells partly by sponging miR-1296.

ZFX promoted the proliferation and motility of pancreatic cancer cells through regulating MAPK signaling.¹⁷ ZFX silencing restrained the proliferation and triggered

the apoptosis of renal carcinoma cells.¹⁹ ZFX promoted the proliferation and elevated the drug resistance of chronic myeloid leukemia cells to imatinib.³³ As for TNBC, CCAT1 contributed to the development of TNBC through upregulating ZFX via acting as a sponge of miR-218,²⁰ indicating the oncogenic role of ZFX in TNBC. ZFX was identified as a target of miR-1296. Furthermore, miR-1296 overexpression-mediated suppressive effects on the malignant behaviors of TNBC cells were largely counteracted by the introduction of pcDNA-ZFX, indicating that miR-1296 suppressed the malignant behaviors of TNBC cells partly by downregulating ZFX. Circ_0000520 can positively regulate ZFX expression by sponging miR-1296 in TNBC cells. We also analyzed the linear relationship among the expression of circ_0000520, miR-1296 and ZFX in TNBC tissues. miR-1296 expression was inversely correlated with the expression of circ_0000520 or ZFX, and there was a positive correlation between the expression of circ_0000520 and ZFX.

Lastly, we assessed the role of circ_0000520 in the xenograft tumor growth in vivo. Circ_0000520 interference significantly suppressed xenograft tumor growth via miR-1296/ZFX axis in vivo. More in vivo experiments need to be conducted to explore the role of circ_0000520 in TNBC tumor metastasis.

In summary, our study found that circ_0000520 promoted the proliferation, migration and invasion and suppressed the apoptosis of TNBC cells through targeting miR-1296/ZFX axis, providing new potential targets for TNBC treatment.

CONFLICT OF INTEREST

The authors declare that they have no financial conflicts of interest.

ORCID

Jing Li  <https://orcid.org/0000-0002-5450-8155>

REFERENCES

- Ahmad A. Breast cancer statistics: recent trends. *Adv Exp Med Biol.* 2019;1152:1–7.
- Navrátil J, Fabian P, Palácová M, Petráková K, Vyzula R, Svoboda M. Triple negative breast Cancer. *Klin Onkol.* 2015;28:405–15.
- Denkert C, Liedtke C, Tutt A, von Minckwitz G. Molecular alterations in triple-negative breast cancer—the road to new treatment strategies. *Lancet.* 2017;389:2430–42.
- Zhang Z, Yang T, Xiao J. Circular RNAs: promising biomarkers for human diseases. *EBioMedicine.* 2018;34:267–74.
- Kristensen LS, Andersen MS, Stagsted LVW, Ebbesen KK, Hansen TB, Kjems J. The biogenesis, biology and characterization of circular RNAs. *Nat Rev Genet.* 2019;20:675–91.
- Kristensen LS, Hansen TB, Venø MT, Kjems J. Circular RNAs in cancer: opportunities and challenges in the field. *Oncogene.* 2018;37:555–65.
- Arnaiz E, Sole C, Manterola L, Iparraguirre L, Otaegui D, Lawrie CH. CircRNAs and cancer: biomarkers and master regulators. *Semin Cancer Biol.* 2019;58:90–9.
- Liu Z, Zhou Y, Liang G, Ling Y, Tan W, Tan L, et al. Circular RNA hsa_circ_001783 regulates breast cancer progression via sponging miR-200c-3p. *Cell Death Dis.* 2019;10:55.

9. Sun H, Tang W, Rong D, Jin H, Fu K, Zhang W, et al. Hsa_circ_0000520, a potential new circular RNA biomarker, is involved in gastric carcinoma. *Cancer Biomark*. 2018;21:299–306.
10. Xu JZ, Shao CC, Wang XJ, Zhao X, Chen JQ, Ouyang YX. circTADA2As suppress breast cancer progression and metastasis via targeting miR-203a-3p/SOCS3 axis. *Cell Death Dis*. et al., 2019;10:175.
11. Hansen TB, Jensen TI, Clausen BH, Bramsen JB, Finsen B, Damgaard CK, et al. Natural RNA circles function as efficient micro-RNA sponges. *Nature*. 2013;495:384–8.
12. Tay Y, Rinn J, Pandolfi PP. The multilayered complexity of ceRNA crosstalk and competition. *Nature*. 2014;505:344–52.
13. Lee YS, Dutta A. MicroRNAs in cancer. *Annu Rev Pathol*. 2009;4:199–227.
14. Chen H, Pan H, Qian Y, Zhou W, Liu X. MiR-25-3p promotes the proliferation of triple negative breast cancer by targeting BTG2. *Mol Cancer*. 2018;17:4.
15. Phan B, Majid S, Ursu S, de Semir D, Nosrati M, Bezrookove V, et al. Tumor suppressor role of microRNA-1296 in triple-negative breast cancer. *Oncotarget*. 2016;7:19519–30.
16. Fabian MR, Sonenberg N, Filipowicz W. Regulation of mRNA translation and stability by microRNAs. *Annu Rev Biochem*. 2010;79:351–79.
17. Song X, Zhu M, Zhang F, Zhang F, Zhang Y, Hu Y, et al. ZFX promotes proliferation and metastasis of pancreatic cancer cells via the MAPK pathway. *Cell Physiol Biochem*. 2018;48:274–84.
18. Li H, Yao G, Zhai J, Hu D, Fan Y. LncRNA FTX promotes proliferation and invasion of gastric Cancer via miR-144/ZFX Axis. *Onco Targets Ther*. 2019;12:11701–13.
19. Fang Q, Fu WH, Yang J, Li X, Zhou ZS, Chen ZW, et al. Knockdown of ZFX suppresses renal carcinoma cell growth and induces apoptosis. *Cancer Genet*. 2014;207:461–6.
20. Han C, Li X, Fan Q, Liu G, Yin J. CCAT1 promotes triple-negative breast cancer progression by suppressing miR-218/ZFX signaling. *Aging*. 2019;11:4858–75.
21. Liu S, Wu M, Peng M. Circ_0000260 regulates the development and deterioration of gastric adenocarcinoma with Cisplatin resistance by Upregulating MMP11 via targeting MiR-129-5p. *Cancer Manag Res*. 2020;12:10505–19.
22. Patop IL, Kadener S. circRNAs in Cancer. *Curr Opin Genet Dev*. 2018;48:121–7.
23. Zhang HD, Jiang LH, Sun DW, Hou JC, Ji ZL. CircRNA: a novel type of biomarker for cancer. *Breast Cancer*. 2018;25:1–7.
24. Meng S, Zhou H, Feng Z, Xu Z, Tang Y, Li P, et al. CircRNA: functions and properties of a novel potential biomarker for cancer. *Mol Cancer*. 2017;16:94.
25. Wang ST, Liu LB, Li XM, Wang YF, Xie PJ, Li Q, et al. Circ-ITCH regulates triple-negative breast cancer progression through the Wnt/ β -catenin pathway. *Neoplasma*. 2019;66:232–9.
26. Wang S, Li Q, Wang Y, Li X, Wang R, Kang Y, et al. Upregulation of circ-UBAP2 predicts poor prognosis and promotes triple-negative breast cancer progression through the miR-661/MTA1 pathway. *Biochem Biophys Res Commun*. 2018;505:996–1002.
27. Qi X, Zhang DH, Wu N, Xiao JH, Wang X, Ma W. ceRNA in cancer: possible functions and clinical implications. *J Med Genet*. 2015;52:710–8.
28. Qu S, Liu Z, Yang X, Zhou J, Yu H, Zhang R, et al. The emerging functions and roles of circular RNAs in cancer. *Cancer Lett*. 2018;414:301–9.
29. Bi J, Liu H, Cai Z, Dong W, Jiang N, Yang M, et al. Circ-BPTF promotes bladder cancer progression and recurrence through the miR-31-5p/RAB27A axis. *Aging*. 2018;10:1964–76.
30. Jia Y, Zhao LM, Bai HY, Zhang C, Dai SL, Lv HL, et al. The tumor-suppressive function of miR-1296-5p by targeting EGFR and CDK6 in gastric cancer. *Biosci Rep*. 2019;39(1):BSR20181556.
31. Chen G, He M, Yin Y, Yan T, Cheng W, Huang Z, et al. miR-1296-5p decreases ERBB2 expression to inhibit the cell proliferation in ERBB2-positive breast cancer. *Cancer Cell Int*. 2017;17:95.
32. Xu Q, Liu X, Liu Z, Zhou Z, Wang Y, Tu J, et al. MicroRNA-1296 inhibits metastasis and epithelial-mesenchymal transition of hepatocellular carcinoma by targeting SRPK1-mediated PI3K/AKT pathway. *Mol Cancer*. 2017;16:103.
33. Wu J, Wei B, Wang Q, Ding Y, Deng Z, Lu X, et al. ZFX facilitates cell proliferation and Imatinib resistance in chronic myeloid leukemia cells. *Cell Biochem Biophys*. 2016;74:277–83.

How to cite this article: Zhou Y, Ma G, Peng S, Tuo M, Li Y, Qin X, et al. Circ_0000520 contributes to triple-negative breast cancer progression through mediating the miR-1296/ZFX axis. *Thorac Cancer*. 2021;12:2427–38. <https://doi.org/10.1111/1759-7714.14085>